⌘ *Author's Choice*

THE JOURNAL OF BIOLOGICAL CHEMISTRY VOL. 284, NO. 32, pp. 21435–21445, August 7, 2009

A Novel "Four-component" Two-component Signal Transduction Mechanism Regulates Developmental Progression in *Myxococcus xanthus*[*][S]

Received for publication, February 24, 2009, and in revised form, June 13, 2009 Published, JBC Papers in Press, June 17, 2009, DOI 10.1074/jbc.M109.033415

Sakthimala Jagadeesan, Petra Mann, Christian W. Schink, and Penelope I. Higgs[1]

From the Department of Ecophysiology, Max Planck Institute for Terrestrial Microbiology, 35043 Marburg, Germany

Histidine-aspartate phosphorelays are employed by two-component signal transduction family proteins to mediate responses to specific signals or stimuli in microorganisms and plants. The RedCDEF proteins constitute a novel signaling system in which four two-component proteins comprising a histidine kinase, a histidine-kinase like protein, and two response regulators function together to regulate progression through the elaborate developmental program of *Myxococcus xanthus*. A combination of *in vivo* phenotypic analyses of in-frame deletions and non-functional point mutations in each gene as well as *in vitro* autophosphorylation and phosphotransfer analyses of recombinant proteins indicate that the RedC histidine kinase protein autophosphorylates and donates a phosphoryl group to the single domain response regulator, RedF, to repress progression through the developmental program. To relieve this developmental repression, RedC instead phosphorylates RedD, a dual receiver response regulator protein. Surprisingly, RedD transfers the phosphoryl group to the histidine kinase-like protein RedE, which itself appears to be incapable of autophosphorylation. Phosphorylation of RedE may render RedE accessible to RedF, where it removes the phosphoryl group from RedF-P, which is otherwise an unusually stable phosphoprotein. These analyses reveal a novel "four-component" signaling mechanism that has probably arisen to temporally coordinate signals controlling the developmental program in *M. xanthus*. The RedCDEF signaling system provides an important example of how the inherent plasticity and modularity of the basic two-component signaling domains comprise a highly adaptable framework well suited to expansion into complex signaling mechanisms.

Two-component signal transduction (TCS)[2] systems are widely employed by bacteria and, to a lesser extent, by eukaryotic microorganisms and plants to mediate adaptive responses to changes in external or internal signals or stimuli. These systems couple a vast array of signals to regulation of highly diverse processes, such as induction of virulence factors, formation of biofilms, sporulation initiation, chemotaxis, quorum sensing, and nutrition utilization (reviewed in Refs. 1–3). The defining feature of these systems is the presence of conserved protein domains that participate in signal transmission via phosphotransfer between histidine and aspartate residues. Specifically, the conserved domains include an HisKA dimerization phospho-accepting domain, which usually contains an invariant histidine as the phospho-accepting residue; a HATPase_c domain, which binds and hydrolyzes ATP to donate the γ-phosphoryl group to the HisKA domain; and a receiver (REC) domain, which contains an invariant aspartic acid as a phospho-accepting domain (reviewed in Ref. 2). These conserved signaling domains are highly modular and can be coupled to a vast variety of signal/stimulus sensing or output domains (4, 5).

TCS systems are named after the most common and simple arrangement of these domains into two components: a histidine protein kinase (HK), in which the HisKA and HATPase_c domains (collectively the transmitter region) are preceded by a variable signal sensing region, and a response regulator (RR) protein in which a REC domain is followed by a variable output (effector) domain (2). In these classical TCS systems, the HK autophosphorylates in response to a change in a specific signal/stimulus, and the phosphoryl group is subsequently transferred to the RR, which then modulates the activity of the associated output domain (2). Typically, the HK and RR genes are encoded together as a pair in a single transcriptional unit.

TCS systems can also consist of more than a single HK and RR pair. In multistep His-Asp phosphorelay systems, an HK first phosphorylates a receiver (REC1) domain, and the phosphoryl group is subsequently passed to a histidine residue contained in an additional histidine-containing phosphotransferase (Hpt)/Spo0B domain. The phosphoryl group is then transferred from the Hpt/Spo0B domain to the receiver (REC2) of the terminal RR, which mediates the adaptive response (6). Histidine phosphotransferase domains alone are not capable of kinase or phosphatase activities. Although Hpt domains share little sequence similarity, structural analyses demonstrate that they share a common four-helix bundle structure in which the phosphorylated histidine lies within a helix (7–9); these characteristics have been used to identify orphan Hpt candidates (10, 11). In these multistep phosphorelay systems, examples exist in which the HK, REC1, and Hpt domains are arranged

* This work was supported by the Max Planck Society and a fellowship from the International Max Planck Research School (to S. J.).

⌘ *Author's Choice*—Final version full access.

[S] The on-line version of this article (available at http://www.jbc.org) contains supplemental Fig. 1 and Tables 1 and 2.

[1] To whom correspondence should be addressed: Karl-von-Frisch-Strasse 1, 35043 Marburg, Germany. Tel.: 49-6421-178301; Fax: 49-6421-178309; E-mail: higgs@mpi-marburg.mpg.de.

[2] The abbreviations used are: TCS, two-component system; HATPase_c, ATPase catalytic domain; HisKA domain, dimerization phospho-accepting domain; REC domain, receiver domain; HK, histidine kinase; RR, response regulator; Hpt, histidine phosphotransferase domain; SMART, Simple Modular Architecture Research Tool; RedD-P and RedF-P, phosphorylated RedD and RedF, respectively; RedC-T, transmitter region of RedC; RedC-T-P, phosphorylated RedC-T; MOPS, 4-morpholinepropanesulfonic acid; Tricine, *N*-[2-hydroxy-1,1-bis(hydroxymethyl)ethyl]glycine.

into the same protein (12) or into two (13, 14) or three (15) separate proteins. In addition to multistep phosphorelay TCS systems, so-called "many-to-one" or "one-to-many" TCS systems (16) have been described in which more than one sensor kinase feeds into a single RR (17, 18), or a single HK functions with more than one cognate RR (19), respectively. These branched systems are thought to be employed to integrate signals into a single output or to coordinate diverse responses to one signal, respectively.

Myxococcus xanthus is a ubiquitous Gram-negative soil-dwelling bacterium with a complex and elaborate multicellular life cycle and is a model organism for complex social behaviors. Under nutrient-rich conditions, *M. xanthus* cells exhibit cooperative feeding (20); the cells swarm in groups and secrete antibiotics and digestive enzymes to paralyze and digest prey microorganisms or digest decaying organic material (21). Under nutrient-limited conditions, *M. xanthus* cells aggregate into mounds (fruiting bodies) of $\sim 10^5$ cells and, within these fruiting bodies, differentiate into environmentally resistant spores (reviewed in Ref. 22). The developmental program requires at least 72 h under laboratory conditions. It is assumed that formation of multicellular spore-filled fruiting bodies aids in the dispersal of groups of spores to more favorable environments such that the spores germinate in groups and cooperative feeding is facilitated. Regulation of the developmental program requires integration of information relating to both individual cells and groups of cells, including starvation status and population density, and requires cells to be both temporally and positionally coordinated (22, 23).

Progression through the *M. xanthus* development program is subject to both positive and negative regulation by TCS systems (listed in Ref. 24). Positive regulators, such as the HKs SdeK (25), AsgA (26), and the RR FruA (27), function to promote developmental progression, and mutants in these genes prevent completion of the developmental program. Interestingly, however, in *M. xanthus*, several TCS signaling systems have been shown to be negative regulators, including EspA (28, 29), TodK (30), EspC (31), and RedCDEF (32). Disruption of these genes causes the cells to progress through the developmental program more quickly, suggesting that the corresponding proteins function to repress progression through the developmental program. This early development phenotype is also associated with the formation of more disorganized, sometimes smaller and more numerous fruiting bodies, and inappropriate sporulation outside of the fruiting bodies, but the sporulation efficiency is not reduced. It is likely that these systems are therefore necessary to ensure coordinated behavior during the complex multicellular developmental program of *M. xanthus*.

In particular, the complex Red signaling system is intriguing, since it consists of four adjacent genes encoding putative two-component signal transduction proteins (*redC*, *-D*, *-E*, and *-F*), which are arranged in a single operon consisting of at least seven genes (*redA* to *-F*) (32). RedC and RedD encode a predicted membrane-bound HK and a dual receiver domain RR, respectively, whereas RedE and RedF encode a histidine kinase-like protein and a single receiver domain RR, respectively. A combination of genetic epistasis and yeast two-hybrid analyses suggests that these four proteins probably function in a single signaling system to regulate progression through the developmental program, but the mechanism of signal transduction is unknown (32).

Here, we employ a combination of genetic and biochemical analyses to characterize each of these four Red TCS proteins. We demonstrate that the HK RedC autophosphorylates and donates a phosphoryl group to the RRs RedF and RedD. Interestingly, the HK-like protein RedE does not appear to autophosphorylate but instead receives a phosphoryl group from the RR RedD and additionally acts as a phosphatase for the RR RedF-P. The phosphorylated form of RedF appears to be abnormally stable *in vitro*. Analysis of the developmental phenotypes of mutants in each gene indicates that RedC and RedF are necessary to repress developmental progression, whereas RedD and RedE are necessary to relieve this repression. These data are assembled into a model of a novel "four-component" signaling mechanism.

EXPERIMENTAL PROCEDURES

Bacterial Strains and Growth Conditions—Bacterial strains and plasmids used in this study are listed in supplemental Table 1. *M. xanthus* strains were grown vegetatively as described previously (29) in CYE broth or agar plates supplemented with 100 μg/ml kanamycin where necessary. *M. xanthus* developmental phenotypes were assayed on CF agar plates as described previously (29). To enumerate spores, triplicate 10-μl spots of culture at 4×10^9 cells/ml were scraped from CF plates after the indicated times of development, and heat- and sonication-resistant spores were isolated and enumerated as described previously (29) except that a Helber bacterial chamber (Hawksley, UK) was used. *Escherichia coli* TOP10 cells were grown under standard laboratory conditions in LB broth (33) supplemented with 100 μg/ml ampicillin or 50 μg/ml kanamycin where necessary.

Construction of M. xanthus Mutant Strains—In-frame deletions and site-specific point mutations were generated by homologous recombination of respective suicide plasmids followed by *galK*-mediated counter selection for loss of the plasmid as described previously (29). Detailed construction of plasmids is described in the supplemental material, and the utilized primers are listed in supplemental Table 2. Strain PH1100 (Δ*redC*) contains the first 31 codons of *redC* fused in frame to the last 24 codons. Strain PH1101 (Δ*redD*) contains the first eight codons of *redD* fused in frame to the last 11 codons, strain PH1102 (Δ*redE*) contains the first seven codons of *redE* fused to the last seven codons, and strain PH1103 (Δ*redF*) contains the first eight codons fused to the last six codons. In strains PH1104 ($redC_{H253A}$) and PH1108 ($redE_{H24A}$), the CAC codons encoding *redC* His 253 and *redE* His 24, respectively, are replaced by a GCG alanine-encoding codon. Strains PH1105 ($redD_{D60A}$), PH1106 ($redD_{D178A}$), and PH1109 ($redF_{D61A}$) contain the GAC codon encoding *redD* Asp-60, *redD* Asp-178, and *redF* Asp-61 codons, respectively, replaced by GCG alanine-encoding codons. Strain PH1107 ($redD_{D60A,D178A}$) was generated by creating the D178A mutation in the PH1105 ($redD_{D60A}$) background. Strain PH1110 (Δ*redDE*) was generated by fusing the first seven codons of *redE* to the last 11 codons of *redD* in the DZ2 (wild type) background. Strain PH1125 ($redC_{H253A}$

Δ*redD*) was generated by creating the Δ*redD* mutation in the PH1104 (*redC*$_{H253A}$) background. Strain PH1126 (*redC*$_{H253A}$ Δ*redF*) was generated by creating the Δ*redF* mutation in the PH1104 (*redC*$_{H253A}$) background. Strain PH1127 (Δ*redD* Δ*redF*) was generated by creating the Δ*redF* mutation in the PH1101 (Δ*redD*) background.

Cloning of Plasmids for Protein Overproduction—Plasmids used for protein overproduction are listed in supplemental Table 1. Sequences of primers used to generate overproduction plasmids are listed in supplemental Table 2. RedC transmitter region (RedC-T) overproduction plasmids pSJ011 and pSJ012 encode the His_6 affinity tag fused at the amino and carboxyl termini of the RedC transmitter region (RedC-T), which constitutes the HisKA and HATPase_c domains, or to the kinase mutant (RedC-T$_{H253A}$), respectively. pSJ011 and pSJ012 were constructed by PCR-amplifying *redC* codons 729–1392 from DZ2 (wild type) or PH1104 (DZ2 *redC*$_{H253A}$) template genomic DNA, respectively. The resulting PCR products were cloned into the EcoRI and SalI sites of pET28a+. Full-length RedC overproduction plasmids pSJ022 and pSJ023 encode RedC with an NH_2-terminal thioredoxin and His_6 tag fused to RedC and RedC$_{H253A}$, respectively. These plasmids were constructed as above except that *redC* was cloned into the EcoRI site of pET32a+. RedD overproduction plasmids pSJ015, pSJ016, pSJ017, and pSJ018, encoding NH_2-terminal thioredoxin and His_6 tags fused to the amino terminus of RedD, RedD$_{D60A}$, RedD$_{D178A}$, or RedD$_{D60A,D178A}$, respectively, were similarly constructed except that *redD* was amplified from DZ2 (wild type), PH1105 (DZ2 *redD*$_{D60A}$), PH1106 (DZ2 *redD*$_{D178A}$), or PH1107 (DZ2 *redD*$_{D60A,D178A}$) genomic DNA templates, respectively, followed by cloning into the EcoRI and SalI sites of pET32a+. RedE overproduction plasmids (pPH133 and pSJ008) encoding a His_6 tag fused to the NH_2 termini of RedE and RedE$_{H24A}$, respectively, were similarly constructed by amplifying *redE* from DZ2 or PH1108 (DZ2 *redE*$_{H24A}$) genomic DNA, respectively, with subsequent cloning into pET28a+. RedF overproduction plasmids (pSJ019 and pSJ020) encoding the NH_2-terminal thioredoxin and His_6 tag fused to RedF and RedF$_{D61A}$, respectively, were similarly constructed by amplifying *redF* from DZ2 or PH1109 (*redF*$_{D61A}$) template genomic DNA, respectively, with subsequent cloning into pET32a+. All constructs were sequenced to confirm the absence of PCR-generated errors.

Overproduction and Purification of Recombinant Proteins—Strains and plasmids used to express recombinant proteins are listed in supplemental Table 1. RedC-T was overproduced in BL21(λDE3) using an overnight autoinduction system (34). RedD or RedE was overproduced in strain BL21(λDE3)/pLysS by induction with 0.5 mM isopropyl 1-thio-β-D-galactopyranoside overnight at 18 °C, or 1 mM isopropyl 1-thio-β-D-galactopyranoside at 37 °C for 3 h, respectively. RedF was overexpressed in strain GJ1158 by induction with NaCl to 0.3 M for 2 h at 37 °C. The respective point-mutated proteins were expressed in the same manner as the wild type parent.

For purification of recombinant proteins, cells were resuspended in binding buffer (50 mM HEPES, 0.5 M NaCl, 20 mM imidazole, pH 7.4) and lysed by a French Press (SLM-AMINCO/Spectronic) three times at ~18,000 p.s.i. Lysate was clarified by centrifugation at 100,000 × *g* for 1 h at 4 °C, and supernatant was filtered (0.45 μm) and then purified by nickel affinity chromatography at 4 °C using an AKTA fast protein liquid chromatograph (Amersham Biosciences) and a 1-ml HisFF1 trap nickel affinity column (Amersham Biosciences). Affinity-tagged proteins were eluted using a 30-ml linear gradient of 20–500 mM imidazole in binding buffer. A portion of each eluted fraction was analyzed by SDS-PAGE. Elution fractions containing peak purified protein were pooled and dialyzed overnight at 4 °C against TGMNKD buffer (50 mM Tris-HCl, pH 8.0, 10% (v/v) glycerol, 5 mM $MgCl_2$, 150 mM NaCl, 50 mM KCl, 1 mM dithiothreitol) (35) for further assays.

Radiolabeled in Vitro Autophosphorylation and Phosphotransfer Assays—In vitro autophosphorylation of 10 μM purified kinase was carried out in 25 μl of TGMNKD buffer (described above) containing 0.5 mM [γ-^{32}P]ATP (14.8 GBq/mmol; Amersham Biosciences) for 30 min as described previously (29) except that 13% polyacrylamide gels were used to resolve radiolabeled proteins.

Radioactive acetyl phosphate was generated by incubating the following reaction at room temperature for 2 h: 1.5 units of acetate kinase (Sigma), TKM buffer (2.5 mM Tris-HCl, pH 7.6, 6 mM potassium acetate, 1 mM $MgCl_2$), and 10 μl of [γ-^{32}P]ATP (14.8 GBq/mmol; Amersham Biosciences) in a total volume of 100 μl. To remove the acetate kinase, the reaction was subject to centrifugation in a Microcon YM-10 centrifugal filter unit (Millipore) for 1 h. The flow-through was collected and stored at 4 °C. To autophosphorylate response regulators, 5 μM response regulator in TGMNKD buffer was incubated with an equivalent volume of acetyl [^{32}P]phosphate for 30 min at room temperature. The reaction was quenched with 2× Laemmli sample buffer (0.125 M Tris-HCl, pH 6.8, 20% glycerol, 4% SDS, 10% β-mercaptoethanol, 0.02% bromphenol blue) (36) and immediately analyzed as above.

Phosphotransfer reactions with purified RedC-T were performed by first autophosphorylating 10 μM RedC-T for 29 min as above. An aliquot was removed for an autophosphorylation control. An equivalent volume containing equal concentration RR was then added to the reaction and incubated for 1 min. Both reactions were then quenched with 2× Laemmli sample buffer to generate 2.5 μM final concentration kinase. A portion of each quenched reaction was analyzed as above.

Kinase-dependent dephosphorylation reactions were performed by first autophosphorylating 5 μM response regulator as described above and then extensively washing the labeled protein with 10 volumes of TGMNKD buffer in Microcon YM-10 filtration columns to remove acetyl [^{32}P]phosphate and ATP. The washing steps normally dilute the response regulators to ~2–2.5 μM. An equivalent volume of 10 μM kinase in TGMNKD buffer (in the presence or absence 1 mM ADP) was then added to the reaction. The reaction was quenched after a 20-min incubation at room temperature and analyzed as above.

Estimation of the phosphorylated half-life of the response regulators was performed by first autophosphorylating 5 μM response regulator and extensively washing as described above. Aliquots were then removed immediately ($T = 0$) and after the indicated times of incubation at room temperature. Each aliquot was immediately quenched as above and stored at −20 °C.

All samples were subsequently resolved as above, and the radioactive signals corresponding to the respective response regulator protein were detected by PhosphorImager analysis. Relative signal intensities were analyzed by Multi Gauge version 3.x (Fujifilm). The Ln values of the background-subtracted average pixel intensity of bands from the PhosphorImager analysis *versus* hours of incubation were plotted, the slope was determined (Microsoft Excel), and the phosphorylation half-lives ($T_{½}$) were determined using the formula $T_{½} = \mathrm{Ln}(2)/-m$, where m is the slope of the intensity *versus* time plot.

Isolation, Autophosphorylation, and Phosphotransfer Experiments with Membrane Fractions—Two-liter cultures expressing RedC, $\mathrm{RedC_{H253A}}$, or the vector control were induced with 0.3 M NaCl overnight at 18 °C in strain GJ1158 bearing plasmids pSJ022, pSJ023, or pET32a+, respectively. Membranes were isolated with modification of a previously described protocol (37). Briefly, harvested cell pellets were washed and resuspended in Buffer B (0.1 M NaH_2PO_4, 10% (v/v) glycerol, 1:20 dilution mammalian protease inhibitor mixture (Sigma), 5 mM EDTA, pH 7.2) and lysed by 2–4 passages though a cell disruptor (Constant Systems) at 2.4 kilobars. Unlysed cells were pelleted at 11,200 × *g* for 10 min, and then membranes were pelleted from the supernatant at 130,000 × *g* for 30 min. Pellets were washed twice with Buffer C (20 mM Tris-HCl, pH 7.8, 5% (v/v) glycerol, 1:20 dilution mammalian protease inhibitor mixture, 1 mM EDTA, 10 mM β-mercaptoethanol) plus 2 M KCl and twice in Buffer C without added KCl and resuspended in 300 μl of Buffer C. All steps were performed on ice or at 4 °C. Membrane preparations were aliquoted and stored at −80 °C.

Autophosphorylation of RedC in membrane fractions was performed by diluting membrane fractions 5-fold into TGMNKD buffer (described above) containing 0.5 mM [γ-^{32}P]ATP (14.8 GBq/mmol), incubating for 4 min, and then quenching samples and processing as described above except that samples were resolved on 15% polyacrylamide gels.

For phosphotransfer reactions, 5 μM RedD proteins or 20 μM RedF proteins were added to diluted membrane fractions, 0.5 mM [γ-^{32}P]ATP was added, and samples were quenched as above after 4 min.

Real Time PCR Analysis—RNA for real time PCR analyses was harvested from cells growing in vegetative conditions ($T = 0$; 4×10^9 cells from CYE broth) or from developing conditions in which 20× 50-μl culture at 4×10^9 cells/ml was spotted onto CF starvation agar plates and harvested by scraping cells off of the agar surface after 12, 24, and 36 h of incubation at 32 °C. Isolation of RNA by the hot phenol method, transcription of cDNA using random hexamer primers, and real time PCR were performed as described previously (29) except that primers specific to *redC* or *espA* were used for real time PCR analysis.

Immunoblot Analysis—Rabbit polyclonal antibodies were generated by Eurogentec (Cologne, Germany) using purified soluble RedC-T, RedF, or RedE protein (as described above) or RedD in gel slices. Preparation of RedD as antigen is described in the supplemental material. All antisera were further purified against the respective antigen using proteins bound to polyvinylidene difluoride membrane (Millipore).

M. xanthus protein lysates for Western blot analyses were prepared from vegetative and developmental cells grown as outlined for real time PCR analysis above. Lysates were prepared from cells pelleted and frozen at −20 °C. Pellets were resuspended in 0.4 ml of MMC buffer (10 mM MOPS, pH 7.6, 4 mM $MgSO_4$, 2 mM $CaCl_2$) containing a 1:20 dilution of mammalian protease inhibitor mixture (Sigma) and disrupted by bead beating (six times for 45 s at 6.5 m/s with 5-min cooling on ice between repeats) in the presence of 0.1-mm Zirconia/Silica beads (Roth) at 4 °C using a FastPrep-24 cell homogenizer (MP Biomedicals). Cell lysates were quantitated using a BCA protein assay (Pierce Thermo Scientific), diluted in 2× Laemmli sample buffer to 1 μg/μl, heated at 99 °C for 10 min, and stored at −20 °C. For immunoblot analysis, 20 μg of protein from cell lysates was resolved by denaturing SDS-PAGE in 13% acrylamide gels (anti-RedD and -RedE immunoblots) or in Tris-Tricine gels (38) except that the separating gel was omitted (anti-RedF immunoblots). Proteins were transferred (39) in a tank system (Hoeffer) to polyvinylidene difluoride membrane. Western blot analyses were performed using all primary antibodies at a dilution of 1:500. Secondary α-rabbit IgG-horseradish peroxidase conjugate antibody (Pierce) was used at a dilution of 1:20,000, and signals were detected with enhanced chemiluminescence substrate (Pierce) followed by exposure to autoradiography film. Representative immunoblot patterns are shown, but similar patterns were obtained from at least two biological replicates.

For Western blots of *E. coli* membrane fraction reactions, samples were prepared as for radiolabeled experiments except that [γ-^{32}P]ATP was omitted. Western blots were performed using anti-mouse penta-His primary antibody (Qiagen) at a 1:1000 dilution according to the manufacturer's instructions. Anti-mouse horseradish peroxidase (Pierce) secondary antibodies were used at a 1:20,000 dilution.

RESULTS

RedC, but Not RedE, Autophosphorylates in Vitro—RedC and RedE are histidine protein kinase homologs proposed to function in the Red TCS system. Typical of most TCS kinase homologs, RedC (470 amino acids) contains a putative membrane-bound sensing region followed by a well conserved transmitter region consisting of a HisKA phosphorylation/dimerization domain (SMART (40, 41) expect value = $4.5\,e^{-11}$) followed by an HATPase_c ATP-binding catalytic domain (SMART expect value = $2.0\,e^{-36}$). The RedC HisKA domain contains an invariant His-253, which is the predicted site of phosphorylation (Fig. 1*A*). In contrast, RedE (242 amino acids) consists solely of a transmitter region containing a poorly conserved HisKA domain (SMART expect value = 2.7) followed by a conserved HATPase_c domain (SMART expect value = $5.3\,e^{-18}$) (Fig. 1*A*). Despite the poor conservation of the HisKA domain, sequence alignments identify an invariant His-24 (data not shown).

To determine whether these proteins autophosphorylate *in vitro*, we set out to overproduce and purify recombinant affinity-tagged RedC and RedE. In the case of RedC, we were unable to overproduce enough full-length protein for purification and therefore instead resorted to purification of the RedC transmitter region (RedC-T; amino acids 243–464). We additionally purified versions of these proteins in which the invariant histi-

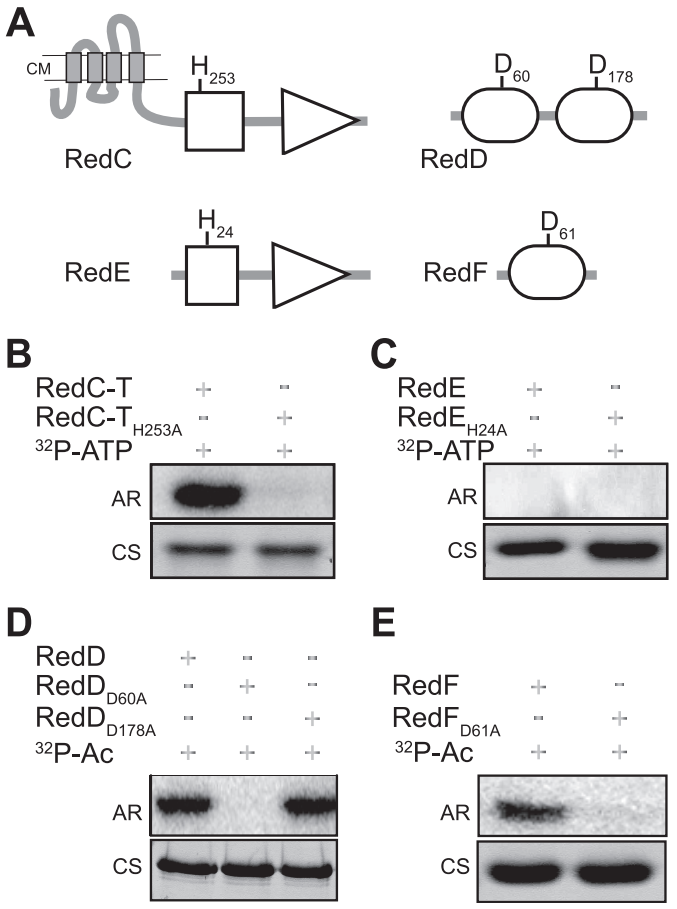

FIGURE 1. *A*, domain architecture of RedC–F two-component signaling homologs. Shown is a schematic diagram of conserved domains detected by SMART (40, 41) in RedC histidine kinase, RedE histidine kinase-like protein, and RedD and RedF response regulator proteins. *Gray rectangles*, transmembrane segments predicted by TMpred Server (available on the World Wide Web); *white squares*, HisKA phosphoaccepting/dimerization domain; *white triangles*, HATPase_c ATP binding and hydrolysis catalytic domain; *white circles*, REC receiver domain. Amino acid positions of the invariant histidine (*H*) and aspartic acid (*D*) residues predicted to be the sites of phosphorylation are identified in the relevant domains. *B–E*, autophosphorylation analysis of Red TCS homologs. Shown are 10 μM purified histidine kinase RedC-T (*B*) or histidine kinase-like RedE (*C*), 5 μM response regulators RedD (*D*) and RedF (*E*), and their respective point mutants. *^{32}P-ATP*, [γ-^{32}P]ATP; *^{32}P-Ac*, [^{32}P]acetyl phosphate; *AR*, autoradiograph; *CS*, Coomassie-stained gel.

dines were substituted with alanines (RedC-T_{H253A} and $RedE_{H24A}$, respectively). When these four proteins were each incubated in the presence of [γ-^{32}P]ATP, RedC-T was efficiently radioactively labeled, whereas RedC-T_{H253A}, RedE, and $RedE_{H24A}$ did not label (Fig. 1, *B* and *C*). Furthermore, RedE and $RedE_{H24A}$ did not become labeled when incubated in reactions in which protein, Mg^{2+}, and ATP concentrations were varied (data not shown). Together, these results indicate that RedC autophosphorylates on its conserved His-253 residue and suggest that RedE may not be capable of autophosphorylation.

RedF and RedD Autophosphorylate in Vitro in the Presence of Acetyl Phosphate—RedD (255 amino acids) is an RR homolog consisting of a fusion of two receiver domains (RedD REC1: SMART expect value = 1.2 e^{-33}; RedD REC2: SMART expect value = 1.9 e^{-25}), whereas RedF is an RR consisting of a single receiver domain (SMART expect value = 2.5 e^{-10}) (Fig. 1*A*). Sequence alignments of the receiver domains of both proteins indicate invariant aspartate residues at positions 60 (Asp-60) and 178 (Asp-178) in RedD and 61 (Asp-61) in RedF. Some response regulators can autophosphorylate *in vitro* when incubated in the presence of small molecule phosphodonors, such as acetyl phosphate (42, 43). To determine if RedD and RedF can autophosphorylate, we purified recombinant affinity-tagged RedD and RedF as well as point mutated versions of these proteins in which the invariant aspartates were mutated to alanine ($RedD_{D60A}$, $RedD_{D178A}$, and $RedF_{D61A}$, respectively). When these proteins were each incubated in the presence of acetyl [^{32}P]phosphate, RedD, $RedD_{D178A}$, and RedF were radioactively labeled, whereas $RedD_{D60A}$ and $RedF_{D61A}$ were not (Fig. 1, *D* and *E*). First, these results indicated that the first receiver domain in RedD appears to autophosphorylate on Asp-60. We cannot, however, distinguish whether Asp-178 in the second receiver domain of RedD does not autophosphorylate in the presence of acetyl phosphate or is only phosphorylated if Asp-60 in the first receiver domain already carries a phosphoryl group. Finally, these results indicated that RedF autophosphorylates *in vitro* on Asp-61.

RedD, RedE, and RedF Are Synthesized under both Vegetative and Developmental Conditions—As a first step to examine the roles of RedC, RedD, RedE, and RedF *in vivo*, we examined their transcriptional and protein accumulation patterns during a developmental time course. Previous data indicated that *redABCDEFG* are co-transcribed in vegetative conditions (32). To determine the developmental transcriptional profile, we examined *redC* by real time PCR at 12, 24, and 36 h of development and plotted the expression level relative to vegetative ($T = 0$) cells. The data obtained suggest that the *red* operon may be slightly down-regulated over the course of a 36-h development (Fig. 2*A*). As a control, we also analyzed the expression of *espA*, which has previously been shown to be up-regulated during development (24, 28, 29).

To determine the expression profile of the RedC, RedD, RedE, and RedF proteins, we generated rabbit polyclonal antibodies against these four proteins. All four affinity-purified antibodies could detect the purified proteins used as antigen (data not shown). However, only anti-RedD, -RedE, and -RedF immunosera could detect the respective proteins in cell lysates. The expression profiles of RedD, RedE, and RedF were essentially similar; proteins were detected under vegetative conditions and during the first 24 h of development, after which the protein levels sharply decreased (Fig. 2*B*). The failure to detect RedC in cell lysates probably arises from a low antibody titer, since reactivity toward even the purified antigen was low in serum from four separate rabbits (data not shown).

Phosphorylated RedF Represses Developmental Progression in Vivo—Previous research demonstrated that deletion of *redEF* was epistatic to deletion of *redCD*, suggesting that RedEF could function downstream to RedCD in a signal transduction pathway (32). To determine whether RedE or RedF is the output of the signaling pathway, we analyzed the developmental phenotypes of mutants bearing single in-frame deletions of either *redE* or *redF*. Δ*redF* mutants began to develop (aggregate into mounds and then sporulate) ~24 h earlier than wild type (Fig. 3), suggesting that RedF is necessary to repress the developmental program. In contrast, Δ*redE* mutants displayed a delayed developmental phenotype, developing ~24 h later than

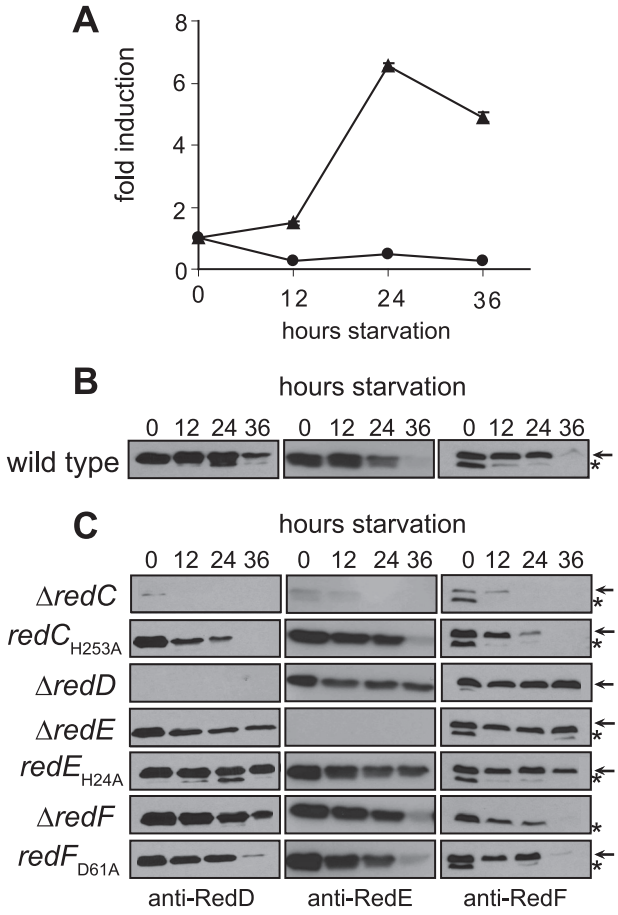

FIGURE 2. **Red expression is observed in vegetative and developmental conditions.** *A*, real time PCR analysis using *redC*-specific (*circles*) and *espA*-specific (*triangles*) primers on cDNA generated from RNA isolated from vegetative cells ($T = 0$) and cells developing on nutrient-limited agar for the indicated times (h). -Fold induction is displayed relative to $T = 0$. *B* and *C*, immunoblot analyses on cell lysates prepared from wild type (DZ2), Δ*redC* (PH1100), $redC_{H253A}$ (PH1104), Δ*redD* (PH1101), Δ*redE* (PH1102), $redE_{H24A}$ (PH1108), Δ*redF* (PH1103), and $redF_{D61A}$ (PH1109) cells harvested as described for *A*, using the indicated antisera. The *arrows* indicate the RedF protein; *asterisks* indicate an unknown protein cross-reacting in the anti-RedF sera.

wild type and displaying a reduction in sporulation to ~30% of wild type levels at 120 h. This phenotype suggests that RedE is required to facilitate developmental progression (Fig. 3). Immunoblot analyses confirmed that RedF and RedE were not detectable in the respective deletion strains (Fig. 2*C*). Importantly, RedD was detected in both deletion strains, and the accumulation of RedE and RedF was not reduced in the Δ*redF* and Δ*redE* strains, respectively (Fig. 2*C*). We can interpolate that RedC is stable in the Δ*redE* and Δ*redF* backgrounds, because RedD accumulated appropriately in both the Δ*redE* and Δ*redF* mutants, whereas RedD fails to accumulate in the Δ*redC* background (Fig. 2*C*).

Interestingly, *redF* mutants phenocopied the Δ*redEF* early development phenotype (Fig. 3), indicating that *redF* is epistatic to *redE* and suggesting that RedF functions downstream of RedE in a signal transduction pathway. In summary, these results suggest that *in vivo* RedF represses developmental progression and RedE acts upstream to RedF to antagonize the function of RedF. To determine whether it is phosphorylated RedF or non-phosphorylated RedF that is necessary to represses the developmental program, we generated the $redF_{D61A}$ point mutation in the endogenous *red* locus and analyzed the associated developmental phenotype. The $redF_{D61A}$ mutant aggregated and sporulated earlier than wild type, similar to the early development phenotype of the Δ*redF* mutant (supplemental Fig. 1). Anti-RedF immunoblot analysis of this strain indicated that the point mutation did not adversely affect the accumulation of RedF, RedD, or RedE (Fig. 2*C*) and implies that RedC is appropriately accumulated as per the reasoning above. These results indicate that if RedF cannot be phosphorylated, development cannot be repressed, indicating that the phosphorylated form of RedF represses development.

RedC Is a Kinase on RedF—The developmental phenotype of the Δ*redE* mutant is inconsistent with that of a mutant in the RedF kinase that would be predicted to share the same early development mutant phenotype as the $redF_{D61A}$ mutant. To confirm that RedE is not the kinase for RedF, we determined that the phenotype of a mutant in which the invariant histidine of RedE was substituted with an alanine ($redE_{H24A}$) displayed a delayed developmental phenotype similar to that of the Δ*redE* mutant (supplemental Fig. 1 and Fig. 3). Immunoblot analysis of this strain demonstrated that the accumulation of $RedE_{H24A}$, RedD, and RedF was not adversely affected (Fig. 2*C*), and this implies that RedC was also produced appropriately (see "Discussion" for reasoning). Together, these results confirm that RedE cannot be a kinase on RedF.

To determine whether RedC could then be the RedF kinase, we next analyzed the developmental phenotype of a Δ*redC* mutant. This mutant developed early (data not shown), but the phenotype cannot be interpreted, since immunoblot analyses revealed that RedD, RedE, and RedF failed to accumulate properly in this strain (Fig. 2, *B* and *C*). We therefore determined that the kinase-inactive $redC_{H253A}$ mutant aggregated and sporulated between 12 and 24 h earlier than wild type and thus has an early development phenotype similar to that of the $redF_{D61A}$ mutant (Fig. 3 and supplemental Fig. 1), which is consistent with the hypothesis that RedC could be the kinase for RedF. Importantly, RedD, RedE, and RedF accumulation was not adversely effected in this mutant (Fig. 2*C*). To determine whether RedC phosphorylates RedF *in vitro*, we first examined phosphotransfer from autophosphorylated RedC-T to RedF or $RedF_{D61A}$. Under these conditions, neither of the RedF proteins was radiolabeled (data not shown), suggesting that either RedC is not a kinase for RedF or that the full-length RedC protein may be required for efficient phosphorylation of RedF.

To distinguish between these possibilities, we assayed for phosphotransfer between full-length RedC and RedF. Although we were unable to overproduce full-length RedC, we isolated membrane fractions from *E. coli* cells expressing low levels of full-length recombinant RedC, $RedC_{H253A}$, or the expression vector alone and incubated them with [γ-^{32}P]ATP. We could detect a specific radiolabeled band corresponding to the expected migration of recombinant RedC, which was absent in the membranes expressing $RedC_{H253A}$ or the vector control (Fig. 4*A*). Anti-His tag polyclonal antibody immunoblot analysis of identical fractions indicated that RedC and $RedC_{H253A}$ were detected at equivalent levels and that no recombinant protein was expressed in the vector control (Fig. 4*A*). These data

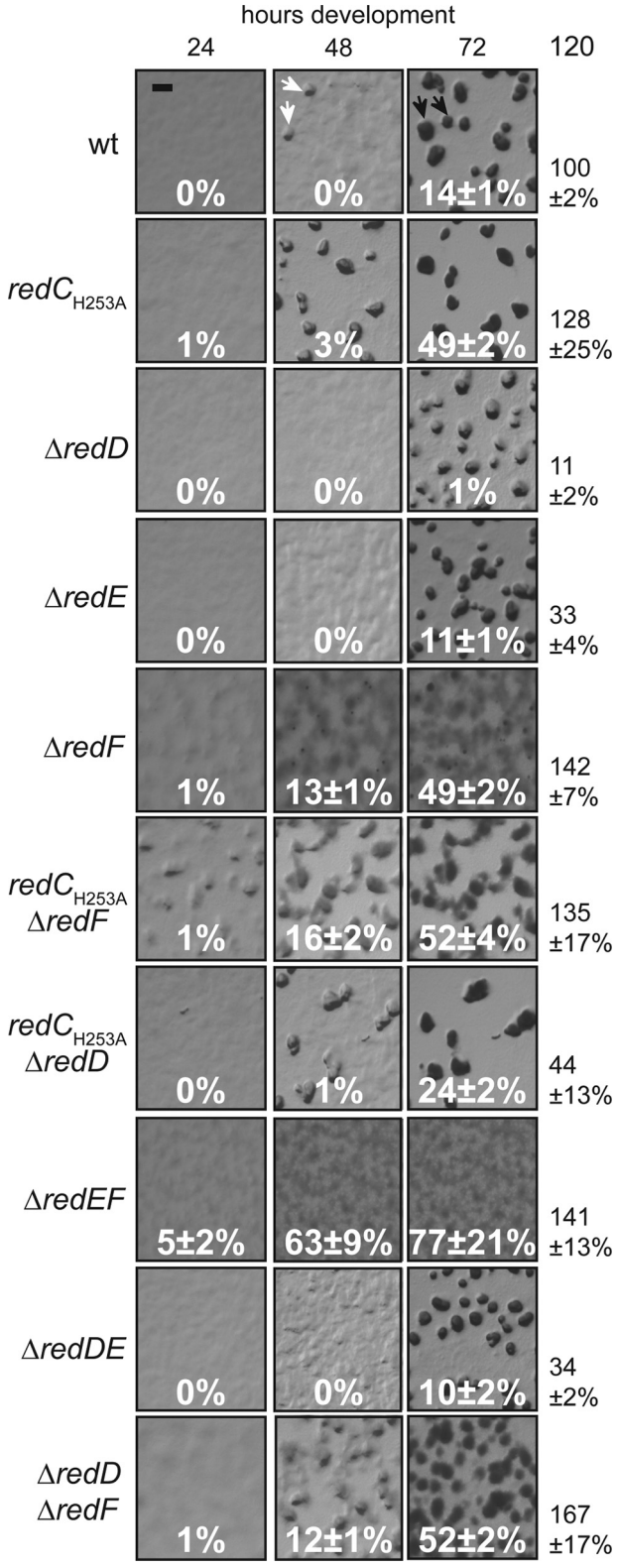

FIGURE 3. **Developmental phenotypes of *red* mutants.** 4×10^7 cells of wild type (DZ2), *redC*$_{H253A}$ (PH1104), Δ*redD* (PH1101), Δ*redE* (PH1102), Δ*redF* (PH1103), *redC*$_{H253A}$ Δ*redF* (PH1126), *redC*$_{H253A}$ Δ*redD* (PH1125), Δ*redEF* (DZ4667), Δ*redDE* (PH1110), or Δ*redD* Δ*redF* (PH1127) strains were spotted on CF nutrient-limited agar and incubated at 32 °C for the indicated times. Cells that are originally plated in confluent layers slowly aggregate into macroscopic translucent mounds (aggregation centers; *white arrows*), which, with the onset of sporulation, darken into fruiting bodies (*black arrows*). In the wild type strain, each fruiting body contains between 10^5 and 10^6 cells (22). Mutant fruiting bodies are often more disorganized and may contain fewer cells. The sporulation efficiency of the developing cells at each time point is displayed *inside* the respective *pictures* for 24–72 h and to the *right* for 120 h. Sporulation efficiencies are calculated as the number of heat- and sonication-resistant spores displayed as a percentage of wild type spores produced at 120 h of development. Reported values are the average and associated S.D. values of triplicate biological replicates. The *bar* in the wild type $T = 24$ *picture* represents 5 mm.

indicate that full-length recombinant RedC in *E. coli* membrane fractions autophosphorylates on His-253, as was previously demonstrated with the purified truncated RedC-T protein (Fig. 1*B*).

We next incubated the same RedC membrane fractions with RedF or RedF$_{D61A}$ in the presence of [γ^{32}P]ATP. Under these conditions, a radiolabeled band corresponding to RedF, but not RedF$_{D61A}$, could be detected (Fig. 4*A*). These radiolabeled bands were not detected if RedF was added to membrane fractions expressing RedC$_{H253A}$ or the vector control (data not shown). Anti-His tag polyclonal antibody immunoblot analysis of identical fractions indicated that RedC and RedF were present in amounts equivalent to those of the respective point mutants in both reactions (Fig. 4*A*). Together, these data indicate that RedC acts as a kinase on RedF in a manner that depends upon the presence of the putative sensing domain.

RedE Acts as a Phosphatase on RedF to Control Developmental Progression—Our genetic analyses suggest that RedE antagonizes RedF-mediated repression of developmental progression. It has previously been demonstrated that certain HKs can also act as phosphatases on their cognate RR, an activity that can be stimulated by the addition of an adenosine nucleoside cofactor (44). To determine whether RedE could act as a phosphatase on RedF-P, we first generated ^{32}P-labeled phosphorylated RedF and then washed it extensively to remove contaminating phosphoryl donors. We then incubated RedF-P alone or with either RedE or RedE$_{H24A}$ in the presence or absence of 1 mM ADP. The radiolabel on RedF-P incubated in the presence of RedE, RedE$_{H24A}$, or only ADP was not diminished compared with RedF-P alone (Fig. 4*B*). However, when RedF-P was incubated in the presence of ADP and either RedE or RedE$_{H24A}$, the radiolabel on RedF was no longer detected (Fig. 4*B*). These results indicate that RedE can act as a phosphatase on RedF-P in a manner dependent upon an ADP (or ATP; data not shown) co-factor. Similar to the bifunctional kinases EnvZ and NtrB, phosphatase activity is not absolutely dependent upon the invariant histidine (45, 46).

We next determined the half-life of phosphorylated RedF, to attempt to explain why RedE could be necessary to antagonize RedF-P. Quantification of the relative signal intensity of radiolabeled RedF-P revealed that RedF was an unusually stable phosphoprotein retaining ~90% of the radiolabel after a 72-h incubation at room temperature (Fig. 5*A*). In contrast, the phosphorylated state of the RedD RR was less stable, with a $T_{½}$ value of ~6 h (Fig. 5*B*).

A Phosphoryl Group Is Transferred from RedD to RedE—Thus far, our results suggested that RedC phosphorylates RedF and RedE dephosphorylates RedF-P. Previous analyses suggested that RedD could interact with both RedC and RedE (32). We therefore first set out to determine whether RedC could phosphorylate

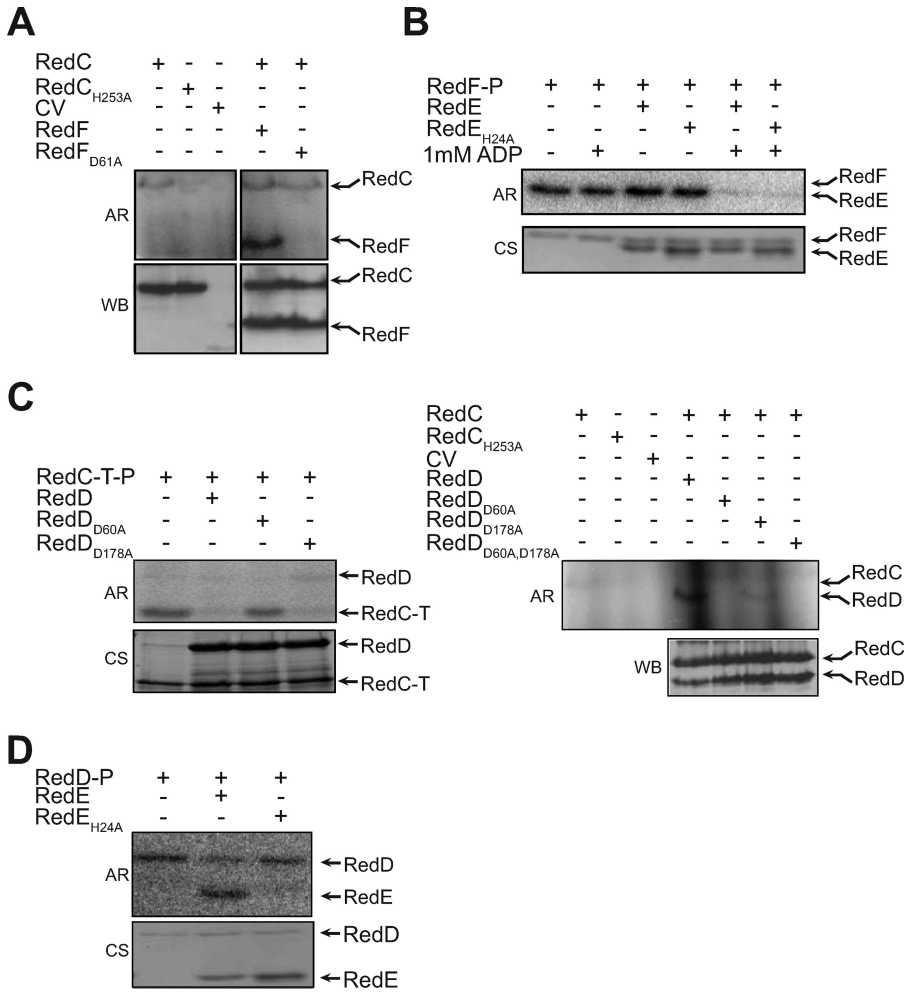

FIGURE 4. ***In vitro* phosphotransfer experiments.** *A*, RedC autophosphorylates and transfers a phosphoryl group to RedF *in vitro*. *Lanes 1–3*, *E. coli* membrane fractions expressing RedC, the kinase-inactive point mutant (RedC$_{H253A}$), or the control vector (*CV*) were incubated with radiolabeled ATP for 4 min. *Lanes 4* and *5*, *E. coli* membrane fractions expressing RedC were incubated in the presence of 20 μM RedF or RedF$_{D61A}$ for 4 min as indicated. *B*, RedE acts as an ADP-dependent phosphatase on phosphorylated RedF. ~2.5 μM RedF-P was incubated for 30 min at room temperature in the absence (−) or presence (+) of 1 mM ADP and/or 5 μM RedE or RedE$_{H24A}$ as indicated. *C*, RedC phosphorylates the first receiver domain of RedD *in vitro*. *Left panel*, autoradiograph of 5 μM autophosphorylated transmitter region of RedC (RedC-T-P) incubated in the absence (−) or presence (+) of 5 μM RedD, RedD$_{D60A}$, or RedD$_{D178A}$, as indicated. *Right*, *lanes 1–3*, *E. coli* membrane fractions expressing RedC, the kinase-inactive point mutant (RedC$_{H253A}$), or the control vector were incubated with radiolabeled ATP for 4 min. *Lanes 4–7*, *E. coli* membrane fractions expressing RedC were incubated with radiolabeled ATP for 4 min in the absence (−) or presence (+) of 5 μM RedD, RedD$_{D60A}$, RedD$_{D178A}$, or RedD$_{D60A,D178A}$, as indicated. *D*, phosphorylated RedD transfers a phosphoryl group to RedE. ~2.5 μM autophosphorylated RedD (*RedD-P*) was incubated for 30 min at room temperature in the absence (−) or presence (+) of 5 μM RedE or RedE$_{H24A}$. *AR*, autoradiograph; *CS*, Coomassie-stained gel; *WB*, anti-His tag Western blot.

RedD *in vitro*. In this assay, we first phosphorylated RedC-T and then incubated it alone or in the presence of RedD. When ^{32}P-radiolabeled RedC-T was incubated in the presence of RedD, radiolabeled RedD protein was not detected, but the radiolabel on RedC-T was significantly reduced (Fig. 4*C*, *left*). This result has two interpretations: 1) RedC-T efficiently phosphorylates RedD, but the rapid intrinsic phosphatase activity of RedD results in loss of the radiolabel from RedD and subsequent depletion of radiolabel from the reaction, or 2) the bifunctional RedC-T phosphorylates RedD and additionally acts as a phosphatase on RedD-P, such that the radiolabel is depleted from the reaction. We favor the latter interpretation, because the addition of RedC to RedD-P results in loss of labeled RedD (data not shown) and because the phosphoryl label on RedD is stable over the course of the 30-min reaction period in the absence of RedC (Figs. 4*C* (*left*) and 5*B*).

To ascertain whether RedC phosphorylates one or both of the two receiver domains of RedD, we next incubated RedC-T-P in the presence of either RedD$_{D60A}$ or RedD$_{D178A}$, which bear substitutions of the invariant aspartate to alanine in the first and second receiver domains of RedD, respectively. The addition of RedD$_{D178A}$ produced the same results as for wild type RedD, whereas the addition of RedD$_{D60A}$ yielded a result that was indistinguishable from RedC-T-P without added RedD (Fig. 4*C*, *left*).

Furthermore, when RedD was incubated with *E. coli* membrane fractions expressing recombinant full-length RedC and [γ-^{32}P]ATP, a RedD-specific radiolabeled band could be readily detected (Fig. 4*C*). A RedD-specific band could not be detected if RedD was incubated with membranes from RedC$_{H253A}$- or vector control-expressing cells (data not shown). When the RedD mutant proteins were incubated in the presence of full-length RedC membrane fractions and [γ-^{32}P]ATP, a weak radiolabel signal could be only detected on RedD$_{D178A}$, whereas RedD$_{D60A}$ and the additional RedD$_{D60A,D178A}$ double mutant control protein did not label. These results suggest that RedC can phosphorylate the first receiver domain of RedD and not the second. Together, these results suggest that *in vitro* RedC can act as both a kinase and a phosphatase on RedD in a manner that could be controlled by the putative sensing domain in RedC.

Because we were unable to generate autophosphorylated RedE, we were unable to test whether RedE also acts as a kinase on RedD. However, we could test whether RedE is also a phosphatase on RedD. We therefore generated phosphorylated RedD and washed the protein extensively to remove small molecule phosphodonors. We then incubated RedD-P alone or in the presence of RedE or RedE$_{H24A}$. In the presence of RedE, but not RedE$_{H24A}$, the radiolabel on RedD was decreased to 73% of the starting RedD-P level (Fig. 4*D*; data not shown). Surprisingly, however, RedE also became radiolabeled, whereas RedE$_{H24A}$ did not. Together, these data suggest that a phosphoryl group is transferred from RedD to the invariant histidine at

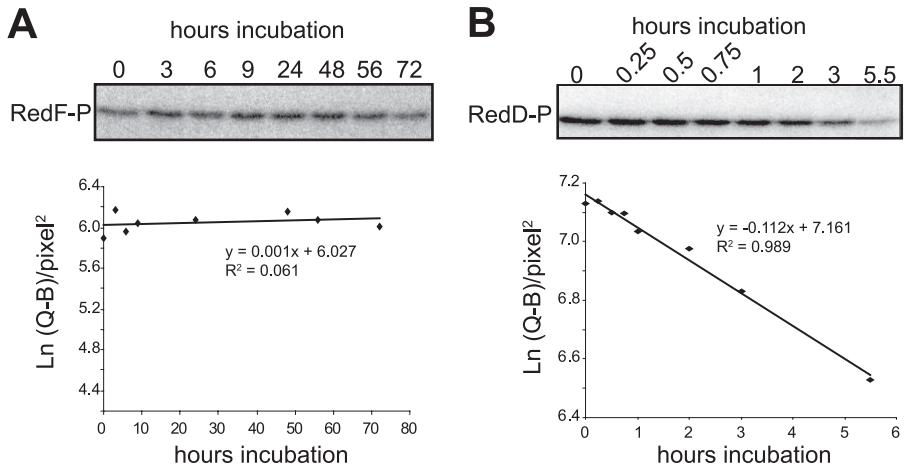

FIGURE 5. **Stability of the phosphoryl group on the RedF and RedD response regulators.** *A*, the *in vitro* phosphorylated form of RedF is stable for greater than 72 h. *Top*, autoradiograph of ~2.5 μM autophosphorylated RedF (*RedF-P*) incubated for the indicated times (h) at room temperature. *Bottom graph*, plot of Ln of average signal intensity of bands from the *panel above versus* time incubation. *B*, the *in vitro* phosphorylated form of RedD has a calculated $T_{1/2}$ of ~6 h. *Top panel*, autoradiograph of ~2.5 μM autophosphorylated RedD (*RedD-P*) incubated for the indicated times (h) at room temperature. *Bottom graph*, plot of Ln of average signal intensity of bands from the *panel above versus* time incubation.

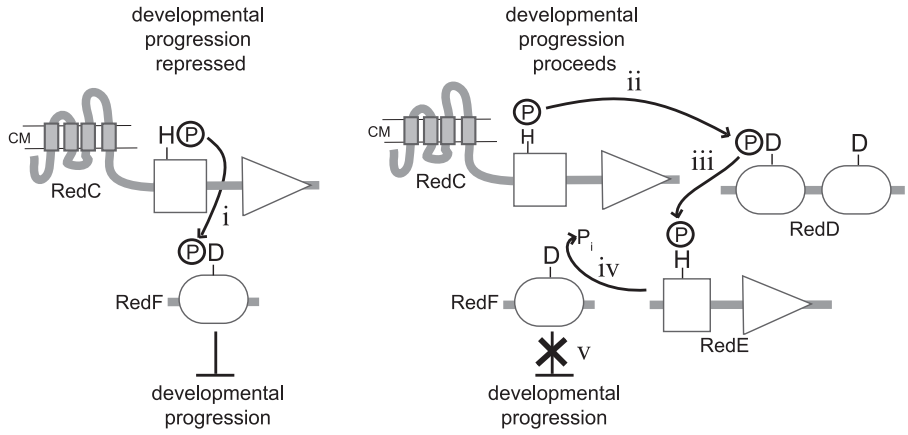

FIGURE 6. **Model for RedCDEF control of developmental progression in *M. xanthus*.** *Left*, repression of developmental progression. Phosphorylated RedF (*RedF-P*) represses progression through the developmental program. RedF is phosphorylated by RedC (*i*). RedD and RedE are present, but their function is not required. *Right*, development proceeds. In response to unknown signals, RedC instead phosphorylates the first receiver domain of RedD (*ii*). The phosphoryl group is passed to RedE (*iii*). RedE removes the phosphoryl group from RedF-P (*iv*), and developmental repression is relieved (*v*).

position 24 of RedE. RedD, therefore, appears to be phosphorylated by RedC and subsequently transfers the phosphoryl group to RedE.

We next sought to clarify the role of RedD in the Red TCS-mediated control over developmental progression *in vivo*. We therefore first investigated the phenotype of a Δ*redD* mutant and found that this mutant exhibited a delayed development phenotype (similar to that of Δ*redE*) but also exhibited an extreme sporulation defect (Fig. 3), suggesting that RedD is necessary to facilitate developmental progression. RedE, RedF, and presumably RedC are stably expressed in the Δ*redD* strain (Fig. 2*C*). Analysis of $redD_{D60A}$, $redD_{D178A}$, and $redD_{D60A,D178A}$ mutants yielded similar delayed development phenotypes (data not shown), but interpretation of these phenotypes is hindered, because anti-RedD immunoblots revealed that the mutant RedD proteins displayed drastic reduction in accumulation *in vivo* (data not shown).

Epistasis Analysis Reveals a Complex Signaling Pathway in Vivo—To further ascertain how these proteins might function together *in vivo*, we analyzed the developmental phenotypes of combinations of individual *red* mutations. The phenotype of a $redC_{H253A}$ Δ*redF* double mutant most closely resembled that of a Δ*redF* mutant, displaying the disorganized fruiting bodies associated with the *redF* phenotype (Fig. 3), indicating that Δ*redF* is epistatic to $redC_{H253A}$ and suggesting that RedF functions downstream to RedC. The $redC_{H253A}$ Δ*redD* mutant displayed a mixed phenotype; it aggregated early like the $redC_{H253A}$ mutant but failed to sporulate properly, achieving only 44% of wild type sporulation efficiency after 120 h of development (Fig. 3). The developmental phenotype of the Δ*redDE* double mutant is that of Δ*redE* (*i.e.* the extreme sporulation defect of the Δ*redD* single mutant is not observed), suggesting that Δ*redE* is epistatic to Δ*redD* and implying that RedD functions upstream to RedE (Fig. 3). Finally, the Δ*redD* Δ*redF* double mutant exhibits the Δ*redF* phenotype (Fig. 3), suggesting that RedF functions downstream to RedD.

DISCUSSION

In this study, we characterized a complex TCS system consisting of four proteins: RedC, a membrane-bound HK; RedD, a dual receiver RR; RedE, an HK-like protein; and RedF, a stand-alone receiver domain. We demonstrated that RedD, RedE, and RedF are expressed both in the vegetative and developmental phases of the *M. xanthus* life cycle. We can indirectly determine that RedC is also present based on the following observations: 1) RedD, RedE, and RedF protein levels are drastically reduced in Δ*redC*, but not $redC_{H253A}$, mutants, and 2) *red* transcript levels are the same in these two mutants (data not shown), indicating that deletion of *redC* does not somehow decrease *red* transcript levels. These observations suggest that RedD, RedE, and RedF are degraded in the absence of RedC. Consequently, if at least RedD, RedE, or RedF is present, RedC is very likely also present.

Using a combination of *in vivo* phenotype analysis and *in vitro* autophosphorylation/phosphotransfer analyses, we propose a model for how these four proteins function together to regulate progression through the developmental program of *M. xanthus* (Fig. 6). A combination of genetic and biochemical data

suggests that repression of the developmental program is mediated by RedC HK-dependent phosphorylation of RedF RR (RedF-P). First, *redC*$_{H253A}$, Δ*redF*, and *redF*$_{D61A}$ mutants display an early developmental phenotype, indicating that RedC kinase activity and phosphorylated RedF are necessary to mediate developmental repression. Second, the *redC*$_{H253A}$ Δ*redF* double mutant displays an early developmental phenotype that is most similar to that of the Δ*redF* mutant. Although both mutants develop early, the Δ*redF* and *redC*$_{H253A}$ Δ*redF* double mutants consistently form darker and more disorganized fruiting bodies than the *redC*$_{H253A}$ mutant, indicating that Δ*redF* is epistatic to *redC*$_{H253A}$ and suggesting that RedF functions downstream to RedC. Finally, recombinant RedC in *E. coli* membrane fractions autophosphorylates and transfers a phosphoryl group to RedF.

Our data suggest that repression of the developmental program is relieved when RedC HK phosphorylates residue Asp-60 on the first receiver domain of RedD RR instead of RedF (Fig. 6). The phosphoryl group is passed from RedD RR to the HK-like RedE protein on His-24, RedE becomes accessible to RedF-P RR, and RedE then removes the phosphoryl group from RedF-P. The evidence for this part of the model is as follows. First, Δ*redE* and Δ*redD* mutants display a delayed developmental phenotype, suggesting that they are necessary to promote the release of developmental repression. Consistent with RedF as the output for the Red system, Δ*redF* is epistatic to both Δ*redE* and Δ*redD* based on the developmental phenotype of the respective double mutants. Second, we observed that *in vitro* both RedC-T-P and full-length RedC phosphorylate RedD REC1, that a phosphoryl group is transferred from RedD-P to RedE His-24, and that RedE acts as a phosphatase on RedF-P.

In our model, RedE is only an efficient phosphatase on RedF-P after it receives a phosphoryl group from RedD-P. First, we observed phosphotransfer from RedD-P to the conserved His-24 in RedE *in vitro*. Second, the *redE*$_{H24A}$ mutant phenocopies the Δ*redE* mutant, indicating that His-24 is essential for RedE function. Third, the phosphatase activity of RedE on RedF-P is not disrupted by the H24A mutation *in vitro*, indicating that phosphorylation is not necessary for phosphatase activity *per se*. Together, these results suggest that *in vivo* RedE is normally not accessible to RedF-P, perhaps because it is sequestered by another protein or differentially localized relative to RedF-P. Phosphorylation of RedE could then release RedE such that it can then act as a phosphatase on RedF-P. Alternatively, it may simply be that the specific activity of RedE-P is higher than that of RedE such that in *in vivo*, RedE does not effectively dephosphorylate RedF-P.

Consistent with the observation that RedE is necessary to release the phosphoryl group from RedF-P, the phosphorylated form of the RedF protein is unusually stable *in vitro*. Our data indicate that ~90% of the radiolabeled phosphoryl group can still be detected on RedF after a 72-h incubation, which means that RedF is the most stable phosphorylated receiver thus far described (47). The intrinsic autodephosphorylation activity of receiver domains varies widely and has been shown to be dependent on the nature of the amino acids located in at least two variable active site residues, and it is generally correlated with the time scale of the biological process being controlled (47). Consistently, the biological process in the case of RedF is control of the lengthy developmental program of *M. xanthus*. We observed that RedF is present not only during vegetative conditions but also up to 30–36 h of development, suggesting that the protein could indeed be functionally active for an extended period of time.

The observation that RedF-P is extremely stable may also explain some of the subtle details of certain *red* mutant phenotypes. For instance, the *redC*$_{H253A}$ mutant has a slightly less severe early development phenotype than the *redF*$_{D61A}$ mutant, suggesting that RedF is phosphorylated at a low level in the *redC*$_{H253A}$ background. Although it is possible that there is an additional minor RedF phosphodonor, which is a genuine input into Red-mediated repression of development, it is also likely that RedF is subject to nonspecific phosphorylation at a low level. The latter interpretation may also explain the mixed early aggregation/reduced sporulation phenotype observed in the *redC*$_{H253A}$ Δ*redD* background; during the long developmental program, nonspecifically phosphorylated RedF would continue to accumulate in the absence of RedD-induced RedE phosphatase activity, and developmental progression could be eventually repressed, leading to the reduced sporulation phenotype.

Our data suggest that the output of the Red system is modulated through the phosphorylation state of RedF, which in turn probably depends upon whether RedC is either phosphorylating RedF or RedD. We do not yet understand the nature of the signal(s) that control this choice, but given the necessity of the NH_2-terminal domain for the RedC-dependent phosphorylation of RedF, the NH_2-terminal region probably constitutes a sensing domain, which, depending upon signal occupancy, could modulate kinase activity and/or the affinity of RedC for either RedF or RedD. A similar observation was made in the three-component CbbRRS TCS system of *Rhodopseudomonas palustris*, in which the NH_2-terminal sensing domain of the HK CbbSR is necessary for determining which of the two RR proteins (CbbRR1 or CbbRR2) becomes phosphorylated (48, 49). It is also conceivable that the second receiver domain in RedD (REC2), for which we have not currently identified a role, is involved in integrating signals from an unidentified histidine protein kinase such that phosphorylation of RedD REC2 could alter the affinity of RedD REC1 for RedC or, alternatively, RedE. Interestingly, sequence alignments of the individual receiver domains of RedD indicate that the two receivers belong to different receiver domain subfamilies, as designated by Grebe and Stock (50). RedD REC1 belongs to receiver class A4 containing NtrC-like RRs, whereas RedD REC2 belongs to family A3 containing CheY-like receiver domains.[3] Interestingly, RedC groups with the NtrB family of kinases (consistent with its role as a kinase for RedD REC1), and we speculate that RedD REC2 could function to integrate signals from an additional TCS system.

An additional important question is how the stand-alone receiver protein RedF could modulate progression through the developmental program. In one scenario, RedF-P could interact with a histidine phosphotransferase and function in a multistep phosphorelay system similar to the role of Spo0F in induction of

[3] S. Huntley and L. Søgaard-Andersen, personal communication.

sporulation in *Bacillus* species. Spo0F is a single domain RR that provides a phosphoryl group to a histidine phosphotransferase protein, which subsequently transfers the phosphoryl group to a DNA-binding RR that directly controls gene transcription (15). Hpt domains can be difficult to identify by sequence alone, and no convincing candidates for the Red system have been identified in *M. xanthus*. In an alternate scenario, RedF could function as an allosteric stimulator of an additional unknown kinase, similar to the effect of DivK of *Caulobacter crescentus* on PleC (51). Finally, RedF could function by directly interacting with an effector protein that modulates the developmental program in a manner analogous to the single domain RR protein CheY, which binds directly to a flagellar switch protein regulating motility via control of the direction of flagellar rotation in chemotaxis systems (52, 53). Although *redC–F* are expressed in an operon containing at least three other genes (*redA*, *redB*, and *redG*), the respective mutants have no detectable phenotypes, suggesting that they are not directly involved in regulating developmental progression (32). We are currently investigating how the developmental program is specifically controlled by the single domain RR RedF and are searching for RedF interaction partners.

Our data suggest an elaborate signaling system that expands the previously described repertoire of two-component signal transduction mechanisms and provides an important example of how the inherent plasticity of the two-component signaling framework can be exploited in different signaling systems. The lengthy multicellular developmental program of *M. xanthus* depends on temporal and positional coordination of intra- and intercellular signals. The Red system is organized such that multiple input signals could be coordinated and integrated, and the presence of a single receiver domain output protein provides the potential for dissemination of signals to several additional systems.

Acknowledgments—We gratefully acknowledge X. Mei for construction of plasmid pSJ023, S. Wegener-Feldbrügge for advice in phosphorylation analyses, C. van der Does and E.-M. Heller for advice with membrane isolation protocols, and L. Søgaard-Andersen, S. Huntley, and S. Wegener-Feldbrügge for helpful discussions. We also gratefully acknowledge L. Søgaard-Andersen, C. van der Does, M. Thanbichler, and K. Thormann for critical reading of the manuscript.

REFERENCES

1. Hoch, J. A., and Silhavy, T. J. (eds) (1995) *Two-component Signal Transduction*, American Society for Microbiology Press, Washington, D. C.
2. Stock, A. M., Robinson, V. L., and Goudreau, P. N. (2000) *Annu. Rev. Biochem.* **69,** 183–215
3. West, A. H., and Stock, A. M. (2001) *Trends Biochem. Sci.* **26,** 369–376
4. Galperin, M. Y. (2006) *J. Bacteriol.* **188,** 4169–4182
5. Mascher, T., Helmann, J. D., and Unden, G. (2006) *Microbiol. Mol. Biol. Rev.* **70,** 910–938
6. Perraud, A. L., Weiss, V., and Gross, R. (1999) *Trends Microbiol.* **7,** 115–120
7. Kato, M., Mizuno, T., Shimizu, T., and Hakoshima, T. (1997) *Cell* **88,** 717–723
8. Song, H. K., Lee, J. Y., Lee, M. G., Moon, J., Min, K., Yang, J. K., and Suh, S. W. (1999) *J. Mol. Biol.* **293,** 753–761
9. Xu, Q., and West, A. H. (1999) *J. Mol. Biol.* **292,** 1039–1050
10. Biondi, E. G., Reisinger, S. J., Skerker, J. M., Arif, M., Perchuk, B. S., Ryan, K. R., and Laub, M. T. (2006) *Nature* **444,** 899–904
11. Biondi, E. G., Skerker, J. M., Arif, M., Prasol, M. S., Perchuk, B. S., and Laub, M. T. (2006) *Mol. Microbiol.* **59,** 386–401
12. Uhl, M. A., and Miller, J. F. (1996) *EMBO J.* **15,** 1028–1036
13. Posas, F., Wurgler-Murphy, S. M., Maeda, T., Witten, E. A., Thai, T. C., and Saito, H. (1996) *Cell* **86,** 865–875
14. Bassler, B. L., Wright, M., Showalter, R. E., and Silverman, M. R. (1993) *Mol. Microbiol.* **9,** 773–786
15. Burbulys, D., Trach, K. A., and Hoch, J. A. (1991) *Cell* **64,** 545–552
16. Skerker, J. M., Prasol, M. S., Perchuk, B. S., Biondi, E. G., and Laub, M. T. (2005) *PLoS Biol.* **3,** e334
17. Jiang, M., Shao, W., Perego, M., and Hoch, J. A. (2000) *Mol. Microbiol.* **38,** 535–542
18. Matsubara, M., Kitaoka, S. I., Takeda, S. I., and Mizuno, T. (2000) *Genes Cells* **5,** 555–569
19. Hess, J. F., Oosawa, K., Kaplan, N., and Simon, M. I. (1988) *Cell* **53,** 79–87
20. Rosenberg, E., Keller, K. H., and Dworkin, M. (1977) *J. Bacteriol.* **129,** 770–777
21. Reichenbach, H. (1999) *Environ. Microbiol.* **1,** 15–21
22. Shimkets, L. J. (1999) *Annu. Rev. Microbiol.* **53,** 525–549
23. Kaiser, D. (2004) *Annu. Rev. Microbiol.* **58,** 75–98
24. Shi, X., Wegener-Feldbrügge, S., Huntley, S., Hamann, N., Hedderich, R., and Søgaard-Andersen, L. (2008) *J. Bacteriol.* **190,** 613–624
25. Pollack, J. S., and Singer, M. (2001) *J. Bacteriol.* **183,** 3589–3596
26. Plamann, L., Li, Y., Cantwell, B., and Mayor, J. (1995) *J. Bacteriol.* **177,** 2014–2020
27. Ellehauge, E., Nørregaard-Madsen, M., and Søgaard-Andersen, L. (1998) *Mol. Microbiol.* **30,** 807–817
28. Cho, K., and Zusman, D. R. (1999) *Mol. Microbiol.* **34,** 714–725
29. Higgs, P. I., Jagadeesan, S., Mann, P., and Zusman, D. R. (2008) *J. Bacteriol.* **190,** 4416–4426
30. Rasmussen, A. A., and Søgaard-Andersen, L. (2003) *J. Bacteriol.* **185,** 5452–5464
31. Lee, B., Higgs, P. I., Zusman, D. R., and Cho, K. (2005) *J. Bacteriol.* **187,** 5029–5031
32. Higgs, P. I., Cho, K., Whitworth, D. E., Evans, L. S., and Zusman, D. R. (2005) *J. Bacteriol.* **187,** 8191–8195
33. Maniatis, T., Fritsch, E. F., and Sambrook, J. (1982) *Molecular Cloning: A Laboratory Manual*, Cold Spring Harbor Laboratory Press, Cold Spring Harbor, NY
34. Studier, F. W. (2005) *Protein Expr. Purif.* **41,** 207–234
35. Rasmussen, A. A., Wegener-Feldbrügge, S., Porter, S. L., Armitage, J. P., and Søgaard-Andersen, L. (2006) *Mol. Microbiol.* **60,** 525–534
36. Laemmli, U. K. (1970) *Nature* **227,** 680–685
37. Williams, S. B., and Stewart, V. (1997) *Mol. Microbiol.* **26,** 911–925
38. Schägger, H., and von Jagow, G. (1987) *Anal. Biochem.* **166,** 368–379
39. Towbin, H., Staehelin, T., and Gordon, J. (1979) *Proc. Natl. Acad. Sci. U.S.A.* **76,** 4350–4354
40. Schultz, J., Milpetz, F., Bork, P., and Ponting, C. P. (1998) *Proc. Natl. Acad. Sci. U.S.A.* **95,** 5857–5864
41. Letunic, I., Copley, R. R., Pils, B., Pinkert, S., Schultz, J., and Bork, P. (2006) *Nucleic Acids Res.* **34,** D257–D260
42. Lukat, G. S., McCleary, W. R., Stock, A. M., and Stock, J. B. (1992) *Proc. Natl. Acad. Sci. U.S.A.* **89,** 718–722
43. McCleary, W. R., and Stock, J. B. (1994) *J. Biol. Chem.* **269,** 31567–31572
44. Zhu, Y., Qin, L., Yoshida, T., and Inouye, M. (2000) *Proc. Natl. Acad. Sci. U.S.A.* **97,** 7808–7813
45. Kamberov, E. S., Atkinson, M. R., Chandran, P., and Ninfa, A. J. (1994) *J. Biol. Chem.* **269,** 28294–28299
46. Hsing, W., and Silhavy, T. J. (1997) *J. Bacteriol.* **179,** 3729–3735
47. Thomas, S. A., Brewster, J. A., and Bourret, R. B. (2008) *Mol. Microbiol.* **69,** 453–465
48. Romagnoli, S., and Tabita, F. R. (2006) *J. Bacteriol.* **188,** 2780–2791
49. Romagnoli, S., and Tabita, F. R. (2007) *J. Bacteriol.* **189,** 325–335
50. Grebe, T. W., and Stock, J. B. (1999) *Adv. Microb. Physiol.* **41,** 139–227
51. Paul, R., Jaeger, T., Abel, S., Wiederkehr, I., Folcher, M., Biondi, E. G., Laub, M. T., and Jenal, U. (2008) *Cell* **133,** 452–461
52. Welch, M., Oosawa, K., Aizawa, S., and Eisenbach, M. (1993) *Proc. Natl. Acad. Sci. U.S.A.* **90,** 8787–8791
53. Szurmant, H., Bunn, M. W., Cannistraro, V. J., and Ordal, G. W. (2003) *J. Biol. Chem.* **278,** 48611–48616